Quantum Hall skyrmions at $\nu = 0, \pm 1$ in monolayer graphene

Thierry Jolicoeur[1] and Bradraj Pandey[2]
[1]*Institut de Physique Théorique, CNRS, Université Paris-Saclay, 91190 Gif sur Yvette, France*
[2]*Laboratoire de Physique Théorique et Modèles statistiques, CNRS, Université Paris-Saclay, 91405 Orsay, France*

(Received 15 July 2019; revised manuscript received 30 August 2019; published 13 September 2019)

Monolayer graphene under a strong perpendicular magnetic field exhibits quantum Hall ferromagnetism with spontaneously broken spin and valley symmetry [K. Nomura and A. H. MacDonald, Phys. Rev. Lett. **96**, 256602 (2006)]. The approximate SU(4) spin/valley symmetry is broken by small lattice-scale effects in the central Landau level corresponding to filling factors $\nu = 0, \pm 1$. Notably, the ground state at $\nu = 0$ is believed to be a canted antiferromagnetic (AF) or a ferromagnetic (F) state depending on the component of the magnetic field parallel to the layer and the strength of small anisotropies. We study the skyrmions for the filling factors $\nu = \pm 1, 0$ by using exact diagonalizations on the spherical geometry. If we neglect anisotropies, we confirm the validity of the standard skyrmion picture generalized to four degrees of freedom. For filling factor $\nu = -1$, the hole skyrmion is an infinite-size valley skyrmion with full spin polarization because it does not feel the anisotropies. The electron skyrmion is also always of infinite size. In the F phase it is always fully polarized, while in the AF phase it undergoes continuous magnetization under increasing Zeeman energy. In the case of $\nu = 0$, the skyrmion is always maximally localized in space both in F and AF phases. In the F phase it is fully polarized, while in the AF phase it has also progressive magnetization with Zeeman energy. The magnetization process is unrelated to the spatial profile of the skyrmions, contrary to the SU(2) case. In all cases, the skyrmion physics is dominated by the competition between anisotropies and Zeeman effect but not directly by the Coulomb interactions, breaking universal scaling with the ratio Zeeman to Coulomb energy.

DOI: 10.1103/PhysRevB.100.115422

I. INTRODUCTION

Monolayer graphene is a new two-dimensional (2D) electron system with Dirac cones in the energy-band structure. Application of a perpendicular magnetic field leads to the formation of Landau levels that have peculiar features not seen in conventional 2D electron gases in semiconducting materials like GaAs. Notably [1–5], at neutrality there are a set of fourfold degenerate Landau levels that stay at zero energy for all values of the field in the absence of Zeeman energy. The graphene physics in this regime is dominated by the interplay between the twofold valley degeneracy and the usual spin degeneracy. This special feature has been clearly observed experimentally [1–4]. It has been shown notably that the fourfold degeneracy is completely lifted, leading to quantum Hall states at Landau level filling factors $\nu = 0, \pm 1$. This phenomenon can be described as a generalization of the quantum Hall ferromagnetism [6] which is well known in the case of the spin degree of freedom [7–17] or in the "which layer" pseudospin for bilayer 2D electron gases [18–20]. In the case of graphene there is an approximate SU(4) symmetry which is spontaneously broken, giving rise to several possible ground states and associated collective Goldstone modes [11].

A general consequence of the formation of quantum Hall ferromagnetic ground states is that charge carriers are now skyrmions instead of simple quasiparticles describable by Hartree-Fock–type electrons or holes. The local extra charge positive or negative is accompanied by a texture in the internal degrees of freedom, i.e., spin and valley in the case of graphene. These entities are well known to appear in the case of SU(2) degeneracy, but the graphene system gives them an even richer structure [21–30]. This is expected to happen close to all integer filling factors. In the case of spin skyrmions, there is a competition between Coulomb interactions and the Zeeman energy: indeed, the interactions favor an extended texture while the Zeeman energy favors localized states. As a consequence, there are a finite number of spin flips in a given texture which can be tuned by varying the ratio of these two energies. This interplay can be captured by Hartree-Fock theory [14,31–40] and exact diagonalization techniques [41–44]. In the case of valley skyrmions, there is no analog of the Zeeman energy so exchange interactions favor infinitely large skyrmions [45]. The case of graphene is richer due to the fact that one may have both spin flips and valley flips. Previous works have investigated this competition for various filling factors. However, there is a crucial ingredient that has to be included: the fact that the SU(4) symmetry is explicitly broken by lattice-scale effects [46–50]. This phenomenon is particularly acute in the central set of states $\nu = \pm 1, 0$. Indeed, at $\nu = 0$ there is a huge degeneracy of SU(4) ground states. To construct a Slater determinant describing $\nu = 0$ according to quantum Hall ferromagnetism theory, one has to select two orthogonal spinors in a four-dimensional space spanned by spin and valley degrees of freedom. This leads [48–52] to candidate states with ferromagnetic (F) or antiferromagnetic (AF) ordering, charge-density wave, or Kekule states all related by the SU(4) symmetry. It is likely that the ground state of monolayer graphene has antiferromagnetic order and that the application of a field parallel to the plane by, e.g., tilting the sample leads to a transition to the ferromagnetic phase and a

change of edge conduction [48,49,53–55]. It is thus important to understand the nature of charge carriers at least in these two phases of graphene in the quantum Hall regime.

In this paper, we use exact diagonalization of small systems in the spherical geometry to study the skyrmion physics. Indeed, it is known that the formation of skyrmions in usual SU(2) systems has very simple observable consequences in this geometry. We show that in the SU(4) case there are no low-energy states beyond those associated with skyrmions generalized to four-flavor case. This is established by formulating counting rules for quantum skyrmion states. We next add anisotropic terms breaking the valley symmetry that is induced by lattice-scale physics. They can be written in a simple form which is parametrized by only two unknown quantities: in addition to an overall strength of the anisotropies, we use an angle whose variation allows to study both AF and F phases.

In the case of filling factor $\nu = -1$, we investigate in detail the electron skyrmion since its hole counterpart does not feel the anisotropies. We find that it is always of infinite size since the ground state has always zero total angular momentum and hence is delocalized over the whole sphere. In the F phase it is also fully spin polarized, but valley totally unpolarized. On the contrary, in the AF phase it undergoes progressive magnetization when increasing the Zeeman energy. In the case of $\nu = 0$, the skyrmion ground state in both phases F and AF prefers to have the maximum angular momentum along the skyrmion branch of states, meaning that it is of smallest possible spatial extent. Again in the F phase it is fully polarized in spin and valley unpolarized while the AF phase also has progressive magnetization and also no valley polarization.

In both cases, the specific feature of these SU(4) skyrmions is that the magnetization process is determined by the energy splitting entirely due to anisotropies within a single-orbital multiplet: $L = 0$ in the case of $\nu = \pm 1$ or $L = L_{\max}$ for $\nu = 0$. This splitting is ruled by the anisotropy energy scale and not by the Coulomb energy scale. Hence, it is a competition between Zeeman effect and anisotropies which governs skyrmion physics.

In Sec. II we recall some relevant facts about monolayer graphene under a magnetic field and the anisotropies important to the physics of the central zero-energy Landau level. In Sec. III we discuss the physics of SU(2) skyrmions in the sphere geometry. In Sec. III we concentrate on the filling factors $\nu = \pm 1$. Section IV is devoted to the filling $\nu = 0$. Finally, Sec. V contains our conclusions.

II. QHE IN MONOLAYER GRAPHENE AND SYMMETRIES

When monolayer graphene is subjected to a perpendicular magnetic field B there is formation of Landau levels which have a simple form close to neutrality:

$$E_{ns} = \mathrm{sgn}(n)\frac{\hbar v_F\sqrt{2}}{\ell_B}\sqrt{|n|} - \frac{1}{2}g_L\mu_B Bs, \tag{1}$$

where n is an integer (positive or negative), the electronic spin is $s = \pm 1$, the magnetic length is given by $\ell_B = \sqrt{\hbar c/eB}$, v_F is the velocity at the Dirac point, μ_B the Bohr magneton, and the Landé factor $g_L = 2$. There is an additional twofold degeneracy due to the two valleys K and K'. Electric neutrality of the graphene layer corresponds to half-filling of the zero-energy Landau level with $n = 0$ in Eq. (1). If we neglect the Zeeman energy $g_L\mu_B B$, there is a fourfold degeneracy. Simple band filling of these Landau levels leads to the prediction of integer quantum Hall effect (IQHE) with Hall conductance:

$$\sigma_{xy} = (4p + 2)\frac{e^2}{h}, \tag{2}$$

with p positive or negative so IQHE occurs at filling factors $\nu = \pm 2, \pm 6, \pm 10, \ldots$. Experiments on high-quality samples have revealed that in fact IQHE occurs at *all* integer filling factors, including the special $\nu = 0$ state. The states at fillings $\nu = \pm 1, 0$ all correspond to some occurrence of quantum Hall ferromagnetism and are the subject of our study. We thus concentrate on the Fock space spanned by the orbital $n = 0$ set of states in the limit of negligible Landau level mixing. Coulomb interactions between electrons are the essential ingredient for quantum Hall ferromagnetism. It is invariant under SU(2) spin rotations but, in fact, there is a larger SU(4) invariance under unitary transformations in the four-dimensional space spanned by the spin and valley degrees of freedom. So, the Hamiltonian we consider contains at least Coulomb interactions and Zeeman energy:

$$\mathcal{H}_0 = \sum_{i<j}\frac{e^2}{\epsilon|\mathbf{r}_i - \mathbf{r}_j|} + \epsilon_Z\sum_i \sigma_i^z, \tag{3}$$

where in the Zeeman term we have used the Pauli matrix σ_z in spin space and $\epsilon_Z = g_L\mu_B B/2$. This symmetry, however, is only approximate and notably the fate of the ground states at $\nu = 0$ depends on details of the graphene system beyond this simple symmetric treatment. The short-distance behavior of Coulomb interactions as well as electron-phonon interactions breaks down SU(4) in a way that can plausibly be modeled by a simple local effective Hamiltonian as proposed notably by Kharitonov [48,49]:

$$\mathcal{H}_{\mathrm{aniso}} = \sum_{i<j}\left[g_\perp\left(\tau_i^x\tau_j^x + \tau_i^y\tau_j^y\right) + g_z\tau_i^z\tau_j^z\right]\delta^{(2)}(\mathbf{r}_i - \mathbf{r}_j), \tag{4}$$

where the τ^α Pauli matrices operate in valley space. The model we consider is given by the total Hamiltonian $\mathcal{H}_0 + \mathcal{H}_{\mathrm{aniso}}$. There is a U(1) symmetry due to rotations around the isospin z axis leading to conservation of the z component of isospin T_z. In the absence of Zeeman energy, there is complete SU(2) spin symmetry which is broken down to U(1) spin rotation around z axis with generator S^z for nonzero Landé factor. The parameters $g_\perp, g_z$ are not precisely known, but the associated energy scale is likely to be larger than the Zeeman energy in graphene samples. This energy scale is nevertheless smaller than the Coulomb energy scale. The main evidence for the role of anisotropies is the presence of a phase transition in the conductance observed when tilting the applied magnetic field [53,55]. It is convenient to parametrize the two coefficients $g_{\perp,z}$ with an angular variable θ:

$$g_\perp = g\cos\theta, \quad g_z = g\sin\theta, \tag{5}$$

in addition to an overall strength g which we take as positive. We next define a dimensionless strength of the anisotropies by using the Coulomb energy scale as a reference point:

$$\tilde{g} = \left(g/\ell_B^2\right)/(e^2/(\epsilon\ell_B)). \tag{6}$$

It is also convenient to translate the parameters $g_{\perp,z}$ into separate energy scales:

$$u_\perp = \frac{g_\perp}{2\pi\ell_B^2}, \quad u_z = \frac{g_z}{2\pi\ell_B^2}. \tag{7}$$

Experimental evidence suggests that the energy scale g/ℓ_B^2 is small compared to the typical Coulomb energy $e^2/(\epsilon\ell_B)$ so the effect of anisotropies should be seen as a small perturbation that lifts SU(4) degeneracies. Notably, it selects the $\nu = 0$ ground state among several possibilities. Let us follow the quantum Hall ferromagnetism approach [48,49,56,57] to describe the filling factor $\nu = 0$. We have to find two orthogonal vectors ϕ_1 and ϕ_2 in the four-dimensional space spanned by $\{|K\uparrow\rangle, |K\downarrow\rangle, |K'\uparrow\rangle, |K'\downarrow\rangle\}$ and fill exactly all orbital indices denoted by m:

$$|\Psi_0\rangle = \prod_m c^\dagger_{m\phi_1} c^\dagger_{m\phi_2}|0\rangle. \tag{8}$$

If we neglect Landau level mixing, then these states, for any choice of the pair ϕ_1, ϕ_2, are exact eigenstates of the fully SU(4) symmetric Coulomb interaction. It is likely that they are even exact ground states as observed numerically on small systems [50]. Adding anisotropies that break the full SU(4) symmetry lifts this degeneracy and leads to the following phases studied in Refs. [48–50]:

(i) The ferromagnetic phase F defined by $\phi_1 = |K\uparrow\rangle$, $\phi_2 = |K'\uparrow\rangle$ which is stabilized in the range $-\pi/4 < \theta < +\pi/2$.

(ii) The antiferromagnetic phase AF with $\phi_1 = |K\uparrow\rangle$, $\phi_2 = |K'\downarrow\rangle$ preferred in the range $\pi/2 < \theta < 3\pi/4$; note that this state is an antiferromagnet both in spin space and in valley space.

(iii) The Kekule state (KD) with $\phi_1 = |\mathbf{n}\uparrow\rangle$, $\phi_2 = |\mathbf{n}\downarrow\rangle$ where $\mathbf{n}$ is a vector lying in the XY plane of the Bloch sphere for valley degrees of freedom: $\mathbf{n} = (|K\rangle + e^{i\phi}|K'\rangle)/\sqrt{2}$ where ϕ is an arbitrary angle in the XY plane. This state is a spin singlet but a XY valley ferromagnet. It is preferred in the range $3\pi/4 < \theta < 5\pi/4$.

(iv) The charge-density-wave state (CDW) defined by $\phi_1 = |K\uparrow\rangle$, $\phi_2 = |K\downarrow\rangle$. This state is a spin singlet but a valley ferromagnet. Since the valley index coincides with the sublattice index in the central Landau level, this state has all the charge density on one sublattice and would be favored by a substrate breaking explicitly the sublattice symmetry like hexagonal boron nitride. It requires the range $5\pi/4 < \theta < 7\pi/4$ as it is stabilized by negative valley interactions along the z direction.

This description is strictly valid in the absence of Zeeman energy. Notably, when the Landé factor is not zero, the AF phase undergoes spin canting: for small Zeeman energy it is energetically more favorable to have the spins lying in the plane orthogonal to the direction of the field and almost antiparallel, both having a small component aligned with the field. Increasing the Zeeman energy leads to an increased component in the field direction up to full saturation where we recover the F phase. A mean-field calculation leads to an approximate state described by $\phi_1 = |K, \mathbf{s}_+\rangle$, $\phi_2 = |K', \mathbf{s}_-\rangle$ with the spin states on the Bloch sphere coordinates are given by $\mathbf{s}_\pm = (\pm\sin\alpha\cos\beta, \pm\sin\alpha\sin\beta, \cos\alpha)$ where β is an arbitrary angle in the XY plane of the spin Bloch sphere and α is the canting angle determined by the competition between Zeeman energy and anisotropies $\cos\alpha = \epsilon_Z/(2|u_\perp|)$. This is the so-called canted antiferromagnetic phase (CAF). Negligible Zeeman energy leads to the pure AF phase while large Zeeman energy realized by tilting the field leads to the limit $\alpha \to \pi/2$: the two spins become aligned and we are in the ferromagnetic phase. The transition observed experimentally in the conductance of the samples of Ref. [53] is attributed to this CAF/F transition. Since we discuss the role of Zeeman energy in some detail, we will use interchangeably AF and CAF for the antiferromagnetic phase.

There are interesting high-symmetry points in the full Hamiltonian $\mathcal{H}_0 + \mathcal{H}_{\text{aniso}}$. They are studied in detail in Ref. [50]. Notably, there is a SO(5) symmetry at the boundary $g_\perp + g_z = 0$ between the AF and the KD phases which unifies antiferromagnetism and Kekule ordering. In this paper, we concentrate on the study of skyrmions only for AF and F phase because these are likely seen in experiments. We note for the future that with a substrate breaking sublattice equivalence (such as hexagonal boron nitride), it is possible to stabilize the KD phase or the CDW phase.

In the case of the filling $\nu = -1$, the ground-state wave function is given by

$$|\Psi_{-1}\rangle = \prod_m c^\dagger_{m\phi}|0\rangle, \tag{9}$$

where ϕ is any spinor and the sum over orbital indices m fills all available states. While this is an exact eigenstate of the SU(4) symmetric Coulomb interactions, it is also an exact eigenstate of the anisotropic Hamiltonian (4) because the wave function (9) vanishes when two particles are at the same point space and the anisotropies are taken to be purely local. It means that the degeneracy in the choice of ϕ is not lifted by the simple model we use. This ambiguity persists for quasihole states that are created from $\nu = -1$ by adding extra flux. Since the state is even less dense than Eq. (9), its wave function still vanishes when particle positions coincide. However, the electron skyrmion which is more dense is sensitive to anisotropies and its fate will be studied in Sec. IV. A lattice model like the one studied in Ref. [58] may be necessary to pinpoint the true nature of the ground state at $\nu = -1$. Since the anisotropies described by Eq. (4) will change the nature of the electron skyrmion for $\nu = -1$, we will refer to the range $\pi/2 < \theta < 3\pi/4$ as the AF phase and $-\pi/4 < \theta < +\pi/2$ as the F phase even for $\nu = \pm 1$.

III. SU(2) SKYRMIONS AND THE SPHERICAL GEOMETRY

In this section we recall basic facts about SU(2) skyrmions as studied in the spherical geometry. We consider electrons with spin $\frac{1}{2}$ interacting through the spin-symmetric Coulomb interaction and no anisotropies in spin space. This means that the Hamiltonian is given by Eq. (3), i.e., it is just $\mathcal{H}_0$. If there are N_ϕ flux quanta through the sphere, then $\nu = 1$ filling of the lowest Landau level requires $N = N_\phi + 1$ electrons and in the absence of Zeeman energy the corresponding wave function is given by a Slater determinant

$$|\Psi_{\nu=1}\rangle = \prod_M c^\dagger_{M\chi}|0\rangle, \tag{10}$$

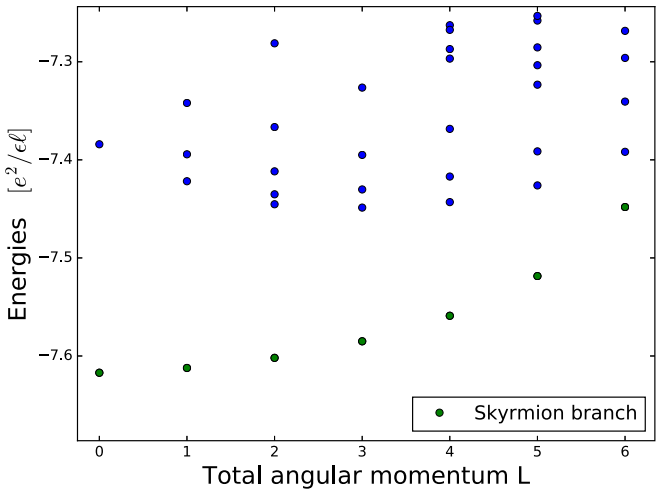

FIG. 1. Energy spectrum of 12 electrons on a sphere with $N_\phi = 12$ flux quanta and zero Zeeman energy, leading to the formation of a SU(2) hole skyrmion. Energies are plotted as a function of total orbital angular momentum. There is a well-defined branch of low-lying states extending from $L = 0$ up to $L = N_\phi/2$ of states having $L = S$ that are interpreted as skyrmion states (green dots). The ground state at $L = 0$ is also a spin-singlet state which is delocalized on the whole sphere. The highest-lying state with $L = N_\phi/2 = 6$ of the skyrmion branch is the fully polarized hole.

where all orbital states are occupied $M = -S, \ldots, +S$ where $N_\phi = 2S$ and $|\chi\rangle$ is *any* spin state. The one-body states indexed by integer or half-integer M are given by

$$\Phi_M^{(S)} = \sqrt{\frac{N_\phi + 1}{4\pi}\binom{N_\phi}{S-M}} u^{S+M} v^{S-M},$$
$$u = \cos\frac{\psi}{2} e^{-i\eta/2}, \quad v = \sin\frac{\psi}{2} e^{i\eta/2}, \tag{11}$$

where ψ, η are spherical coordinates and the number of flux quanta through the sphere $N_\phi = 2S$ is an integer. One-body states are eigenstates of the orbital angular momentum and so many-body states can also be classified with total angular momentum since Coulomb interactions and local anisotropies translate into rotationally invariant interactions on the sphere. The state wave function (10) is an orbital singlet $L_{\rm tot} = 0$ and a ferromagnetic multiplet of maximal total spin since the state is totally spin symmetric. From this fiducial state one can now add or remove one electron to obtain an entity carrying charge. A Hartree-Fock approximation is simply to remove one electron from wave function (10) or to add an electron with a spin state χ' orthogonal to χ and in any orbital state. Indeed, the ground states are no longer exactly given by a simple Slater determinant.

It has been discovered numerically [8,9] that the ground state becomes a spin and orbital singlet when changing by one unit the number of charges in the system. In addition to a $L_{\rm tot} = S_{\rm tot} = 0$ ground state, there is a low-lying well-defined branch of states that have equal spin and orbital momentum $L = S$ that rises up to $L = S = N_\phi/2$. It is well isolated from higher-lying states (see Fig. 1 for a typical spectrum in the absence of Zeeman energy). The end of this skyrmion branch is reached for $L = N_\phi/2$ by the fully polarized hole state whose exact wave function can be obtained by removing one creation operator in the wave function (10). This skyrmion branch is the finite-size translation of the skyrmion spin texture described by the nonlinear sigma model [10,11]. The shape of the branch is a reflection of interaction potential between electrons. Indeed, by using a hard-core interaction between same-spin electrons, it becomes perfectly flat.

It is convenient to introduce the number of overturned spins K with respect to the fully polarized case by $L = S = N_\phi/2 - K$: K increases monotonically as we go along the skyrmion branch starting from the polarized hole with $K = 0$. The ground state with $L = 0$ is fully delocalized on the sphere and corresponds to a skyrmion of infinite size in the thermodynamic limit. It is reached for larger and larger K as the number of particles grows. The exponential growth of the Fock space with the number of particles severely limits the sizes that can be reached by exact diagonalization. It means we can study only skyrmions with a small number of overturned spins. To overcome this problem, it is also possible to use trial wave functions in Hartree-Fock calculations. They can written in the disk geometry as follows:

$$|\Psi_h\rangle = \prod_{m=0}^{\infty} \left(u_m c_{m\uparrow}^\dagger + v_m c_{m+1\downarrow}^\dagger\right)|0\rangle, \tag{12}$$

where the one-body states indexed by a positive integer m are the symmetric gauge lowest Landau level eigenstates:

$$\phi_m(z) = \frac{z^m}{\sqrt{2\pi\, 2^m m!}} \exp\left(-|z|^2/4\ell_B^2\right), \tag{13}$$

where we have defined the complex planar coordinate $z = x + iy$ and $m \geqslant 0$ is a positive integer. The coefficients u_m and v_m are variational parameters.

The magnetization process of the skyrmion involves both spin and orbital angular momentum. In the absence of the Zeeman term, the ground state is the $L = 0$ member of the skyrmion branch. This describes a state with no characteristic length scale; it is delocalized over all the sphere and corresponds to a skyrmion of infinite size. With finite Zeeman coupling all higher-lying states along the skyrmion branch are split according to their spin value: since for a finite system there are finite-energy separations between these states there will be a succession of level crossings when states with increasing spin become the ground state in the presence of the Zeeman effect. The magnetization curve is then a staircase as a function of the applied field B. The critical fields are defined through

$$g_L \mu_B B_{\rm crit}^{(N/2-K)} = E_{L=K+1} - E_{L=K}. \tag{14}$$

See, e.g., Fig. 2 where we plot the number of overturned spins K with respect to the fully saturated case. It is only beyond some critical field that the ground state becomes fully magnetized when a state from the multiplet with $L = N_\phi/2$ becomes the ground state. If we apply the Hartree-Fock (HF) method to the state (12) along the lines of Refs. [13,14,31,32,40], we obtain another approximation to the skyrmion state and thus of the magnetization curve. In Fig. 2 we have plotted the HF result in addition to the curve extracted from exact diagonalization with 12 electrons on a sphere. We recover the typical skyrmion spin flip of $K \approx 3$ when $g_L \mu_B B \approx 0.015 e^2/(\epsilon \ell_B)$

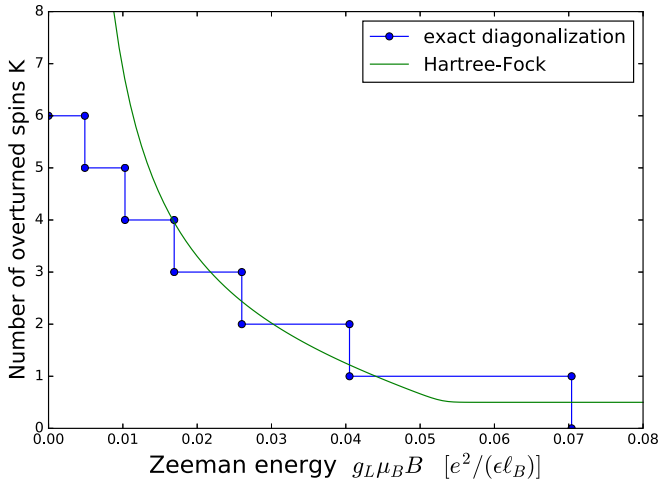

FIG. 2. The number of overturned spins in a SU(2) hole skyrmion as a function of Zeeman energy. The blue steps indicate the level crossings as observed by exact diagonalization of $N = 12$ electrons on a sphere with $N_\phi = 12$. The green curve comes from a Hartree-Fock calculation with the variational state (12). A finite Zeeman energy is required to fully polarize the system.

in GaAs systems. The various approaches to the skyrmion properties have been compared in Ref. [12]. It is important to note that the Coulomb interaction is responsible for the shape of the skyrmion branch and there is a competition between this effect and the Zeeman energy to determine the skyrmion profile. This simple picture will break down in the SU(4) case as we discuss in the following.

IV. SKYRMIONS AT $\nu = \pm 1$

If we first neglect anisotropies, we can make exact statements about SU(4) skyrmions at filling factor $\nu = -1$ and its particle-hole partner filling $\nu = +1$. Indeed, if we consider exact eigenstates of the SU(2)-symmetric situation without Zeeman coupling, these states can be embedded in the larger Fock space built for four flavors and since Coulomb interactions are fully SU(4) symmetric, these states will remain exact eigenstates. The only characteristic that changes is the degeneracy since one spin flip is exactly equivalent to any flavor flip, only the counting of states is different. So, we know that the SU(2) skyrmion states are still present in the SU(4) case. The only question is whether or not intruder states will destroy this picture. This question can be studied by our exact diagonalizations and the answer is simple: there are no new intruder states with SU(4) character beyond the states we know from the SU(2) case. We find that this is valid for the whole skyrmion branch: the picture corresponding to our Fig. 1 is thus exactly the same in the SU(4) case. Only the degeneracies of the states change. There are of course additional new states but they lie at higher energies in the upper part of the spectrum. This is evidence for the correctness of the discussion given in Ref. [21]. These arguments equally apply to $\nu = \pm 1$ and $\nu = 0$.

According to Refs. [6,21], the degeneracies can be computed straightforwardly with Young tableaux. The skyrmion state with largest angular momentum spans an SU(4) irreducible representation (IR) given by one row of N_ϕ boxes:

$$L = N_\phi/2 \ : \quad \underbrace{\square\square\cdots\square}_{N_\phi} \ ; \tag{15}$$

then the neighboring state with $K = 1$ has one row of $N_\phi - 1$ boxes and one row of one box:

$$L = N_\phi/2 - 1 \ : \quad \begin{array}{l}\square\square\cdots\square\\ \square\end{array} \ . \tag{16}$$

We move then along the whole skyrmion branch by removing boxes from the upper row and transferring them to the second row :

$$L = N_\phi/2 - 2 \ : \quad \begin{array}{l}\square\square\cdots\square\\ \square\square\end{array} \ . \tag{17}$$

We proceed until there are $N_\phi/2$ boxes in both rows (we assume N_ϕ even for simplicity, otherwise there is one remaining box):

$$L = 0 \ : \quad \begin{array}{l}\square\square\cdots\square\\ \square\square\cdots\square\end{array} \ . \tag{18}$$

In the SU(2) case, we can omit the second row and we just obtain the spin multiplets with $L = S$. In the SU(4) case, these IRs have dimensions given by

$$\mathcal{D}(a,b) = \tfrac{1}{2}(a+1)(b+1)(b+2)(a+b+2)(a+b+3), \tag{19}$$

where b is the number of columns with two boxes and a is the number of columns with one box.

We now turn to the role of graphene-specific anisotropies at $\nu = \pm 1$. In the absence of the Zeeman term, eigenstates are classified by total angular momentum and spin as in the SU(2) case, but the anisotropic Hamiltonian (4) allows conservation of valley isospin along the z direction. The corresponding isospin T_z is a good quantum number that we use in our exact diagonalizations in addition to L_z and S_z. This is for a generic angle: special values of θ in Eq. (4) have more conserved quantities which we do not consider here. As long as the magnitude $\tilde{g}$ of the anisotropy remains small, each state of the skyrmion will have its SU(4) degeneracy lifted but the overall picture remains valid. In Fig. 3 we have plotted the spectrum of a 10-electron system with flux tuned to create an electron skyrmion. The states of the skyrmion branch are now split in a series of multiplets and, for small enough anisotropy, they still keep the shape we associate to skyrmion states from the SU(2) case. Even for an unrealistically large value of $g/\ell_B^2 = e^2/(\epsilon\ell_B)$ the skyrmion survives. The effect of anisotropies of Eq. (4) for small $\tilde{g}$ is simply a first-order perturbation theory lifting the degeneracies between members of a given L multiplet. The eigenstates with nonzero anisotropies still have good quantum numbers: total spin and also T_z. But now we have to take into account the fact that the magnetization process that takes place when we increase the Zeeman energy is quite different from what happens in the SU(2) discussed in Sec. III. Indeed, for each multiplet along the skyrmion branch there are states with all possible values of the spin form $S = 0$ up to $S = N/2$. So, each multiplet has its own magnetization

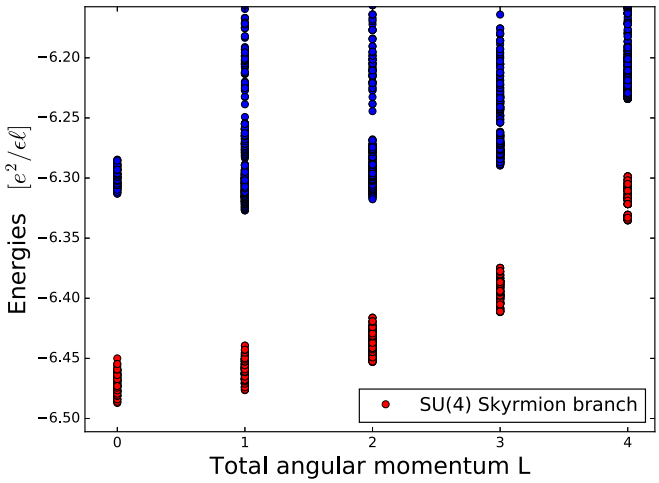

FIG. 3. Energy spectrum of 10 electrons on a sphere with $N_\phi = 8$ flux quanta and zero Zeeman energy. There is formation of a $\nu = -1$ electron skyrmion. Energies are plotted as a function of the total angular momentum. The anisotropies are taken to be $\tilde{g} = 0.1$ and the anisotropy angle is $\theta = 0.6\pi$ so the system is in the AF phase. All SU(4) multiplets along the skyrmion branch are now split into manifolds of states with an energy splitting scale $O(\tilde{g})$ [even with a very large anisotropy $O(1)$ the skyrmion picture is not destroyed]. The value $\tilde{g} = 0.1$ is chosen for readability of the figure, and realistic values are likely smaller.

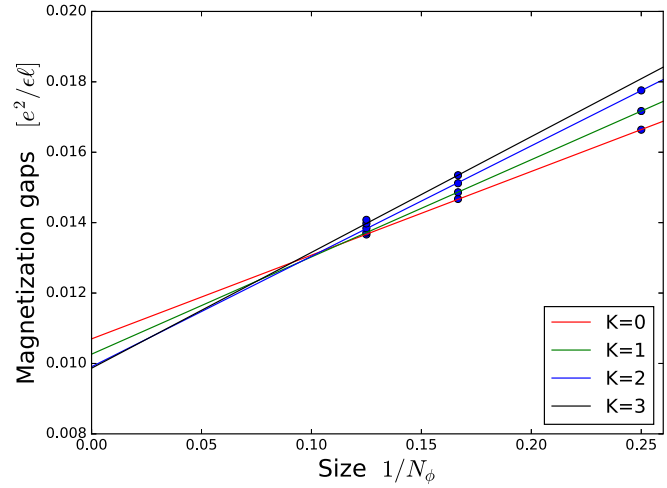

FIG. 4. The gaps between the singlet state and the fully magnetized state for a given K value as a function of system size. The values are computed in the AF phase with $\theta = 0.6\pi$ and $\tilde{g} = 0.1$. The tentative linear fits given by the straight lines are listed in Table I.

curve and thus one has to figure out which multiplet will describe the magnetization process in the thermodynamic limit. An important consequence is that the energy scale of the magnetization curve is set by the anisotropy energies and not by the Coulomb scale :

$$g_L \mu_B B_{\rm crit}^{(S)} = E_{S+1} - E_S = O\big(g/\ell_B^2\big). \tag{20}$$

This is due to the fact that all level crossings corresponding to the magnetization process occur within a manifold of states whose degeneracy is lifted solely by nonzero anisotropies.

We now discuss the level ordering in the two phases of interest, AF and F. The situation in the F phase is very simple indeed: for each value of L, the multiplet has a ground state with the maximal spin $S = N/2$ as can be guessed by the ferromagnetic nature of the anisotropies. As a consequence, the maximal spin state with $L = 0$ will be the ground state for *all* values of the Zeeman energy. This means that in the F phase the skyrmions are always of infinite size and always fully polarized for all values of the Zeeman field. This is very different from the case of SU(2) skyrmions where the fully polarized quasiparticle is the state which is maximally localized with a size of order ℓ_B. Concerning the valley degrees of freedom, the ground state has always the smallest possible value of T_z, i.e., $T_z = 0$ for N even and $T_z = \frac{1}{2}$ for N odd. So, the skyrmion is valley unpolarized.

We have checked that this picture is valid deep in the F phase but we cannot track the eigenstates close to the transition point $\theta = \pi/2$ because there are additional degeneracies due to the enhanced symmetry rendering delicate the convergence of Krylov-subspace methods.

In the AF phase, we observe now that the ordering of the multiplets is reversed with respect to the F case and now the ground state at fixed L has always zero spin. The magnetized states have energies increasing with magnetization at fixed L. It is convenient to index states along the skyrmion branch again by $K = N_\phi/2 - L$, $K = 0, 1, \ldots$. For each K we define the magnetization gap $G_{N_\phi}(K)$ as the difference in energy between the ground state at this K and the lowest-lying state which is fully polarized and hence has a spin $S = N/2$, however, this spin value is now unrelated to K, contrary to SU(2) skyrmions. These gaps are plotted in Fig. 4 as a function of $N_\phi = 4, 6, 8$ for the accessible values of K. They converge to a nonzero value in the thermodynamic limit $G(K)$ which we estimate by linear fits in Table I. They are expected to be $O(\tilde{g})$ for small $\tilde{g}$. We observe that $G(K)$ is decreasing monotonously toward a nonzero value with increasing K. This means that if we consider the effect of the Zeeman splitting, the lowest levels will always be those from the $L = 0$ set of states. In Fig. 5 the Zeeman splitting of the $L = 0$ and 1 states of the largest system we could reach with 12 electrons is displayed. We have taken into account only the lowest-lying states with increasing spin and added a Zeeman coupling only to states whose energy decreases with the field for clarity. The lower envelope of the set of curves is entirely due to the states coming from the $L = 0$ multiplets. It is precisely this envelope that determines the magnetization curve. So, the magnetization process is entirely due to the $L = 0$ multiplet.

TABLE I. Estimates of the gaps between the spin-singlet ground state at fixed K value and the lowest-lying fully spin-polarized state. Gaps are given in units of the Coulomb scale $e^2/(\epsilon\ell_B)$ and parameters are the same in Fig. 4: $\theta = 0.6\pi$ and $\tilde{g} = 0.1$.

K	Magnetization gap $G(K)$
0	0.0107
1	0.0102
2	0.0099
3	0.00985

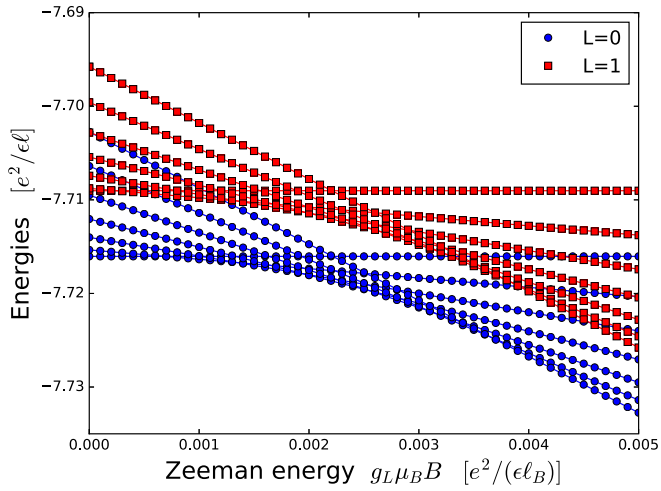

FIG. 5. Evolution of energy levels of a 10-electron system with an electron skyrmion due to Zeeman effect: we have plotted only levels with spin ranging from $S = 0$ up to the maximal value $S = N/2$ and for clarity followed only the levels with largest S^z value of each multiplet: these are the states that have the largest slope as a function of B. Blue traces belong to the multiplet of states with $L = 0$, while red traces are coming from the $L = 1$ multiplet. So, the magnetization is always entirely due to the $L = 0$ states. The envelope of these states determines the magnetization process of the skyrmion. Our finite-size studies show that this is still the case in the thermodynamic limit.

We plot in Fig. 6 the magnetization process for a system of 10 electrons at $N_\phi = 8$. All energy scales are proportional to $\tilde{g}$ for small $\tilde{g}$, so with data for $N_\phi = 4, 6, 8$ this means that the critical Zeeman energy to fully saturate the system is $\approx 0.05\tilde{g}$ in units of the Coulomb energy. It is important to note that due to the special magnetization process as deduced from Eq. (20), the magnetization curve is proportional to $\tilde{g}$ (as long as $\tilde{g} \lesssim 1$) so it is universal with respect to the magnitude of the anisotropies. Of course, it still depends upon the value of θ.

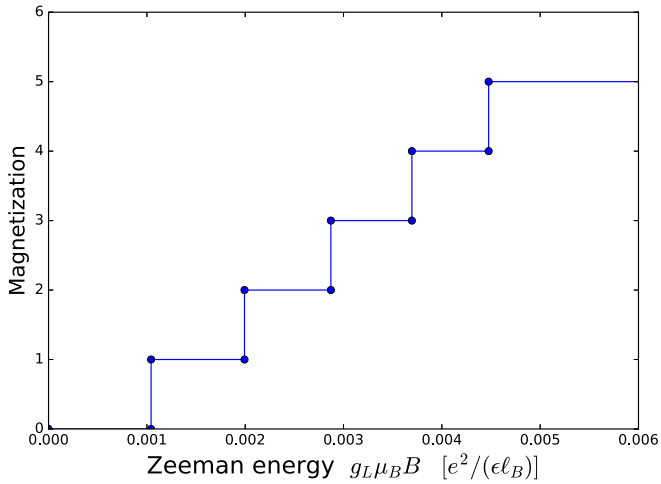

FIG. 6. The magnetization of the set of $L = 0$ states for the electron skyrmion at $N_\phi = 8$ in the AF phase with $\theta = 0.6\pi$ and $\tilde{g} = 0.1$. Note that this staircase curve will collapse onto the vertical axis when we reach the F phase for $\theta = 0.5\pi$.

The AF skyrmion is thus of infinite size, is valley unpolarized because all relevant states have also the minimal allowed value of T_z, and requires a critical Zeeman energy to be fully polarized:

$$g_L\mu_B B_{\text{crit}} \approx 0.05\left(g/\ell_B^2\right). \tag{21}$$

V. SKYRMIONS AT $\nu = 0$

We now discuss the fate of the skyrmion excitations at filling factor $\nu = 0$. The ground state at $\nu = 0$ is described by the wave function (8). The corresponding SU(4) IR is described by a Young tableau with two rows of equal length (when N_ϕ is even). We consider now only the case of the hole skyrmion because for $\nu = 0$ it is related to the electron skyrmion by particle-hole symmetry. If we want to create a skyrmion, the recipe proposed by Ref. [6] is to glue an additional row of boxes describing a full inert shell on top of the Young tableaux describing the skyrmion branch of $\nu = \pm 1$. So, the member of the branch with maximal L belongs to the IR:

$L = N_\phi/2$: 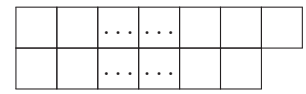 (22)

with the $N_\phi + 1$ boxes in the top row and N_ϕ boxes in the lower row. We now move along the skyrmion branch with decreasing L by moving boxes from the second row to a third row:

$L = N_\phi/2 - 1$: 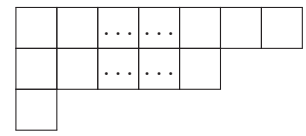 . (23)

For a state with $L = N_\phi - K$, the top row always has $N_\phi + 1$ boxes, the second row has $N_\phi - K$ boxes, and the third row K boxes. We have checked that the multiplicities of the states we find from our exact diagonalization (ED) calculations are exactly reproduced by the dimension of these IRs. An example spectrum is given in Fig. 7. As in the $\nu = \pm 1$ case, addition of anisotropies lifts the degeneracies and does not blur the overall picture for $\tilde{g}$ up to unity. However, we observe a unique phenomenon: the ground state of the skyrmion branch does not stay at $L = 0$ even in the absence of Zeeman energy (see Fig. 8). In fact, increasing the strength $\tilde{g}$ shifts the ground state to larger and larger values of L at fixed size N_ϕ. This means that the skyrmion has no longer a finite size due to anisotropies in line with the arguments presented in Ref. [24]. For $\tilde{g}$ large enough, the ground state has the smallest allowed size of order ℓ_B for the maximum L of the branch. In Tables II and III we

TABLE II. The angular momentum of the ground state of a skyrmion state with $N_\phi = 4$ and $N = 9$ electrons as a function of anisotropy scale $\tilde{g}$ for $\theta = 0.6\pi$.

$\tilde{g}$	0.1	0.2	0.3	0.4	0.5	0.6
L	0	0	1	1	1	2

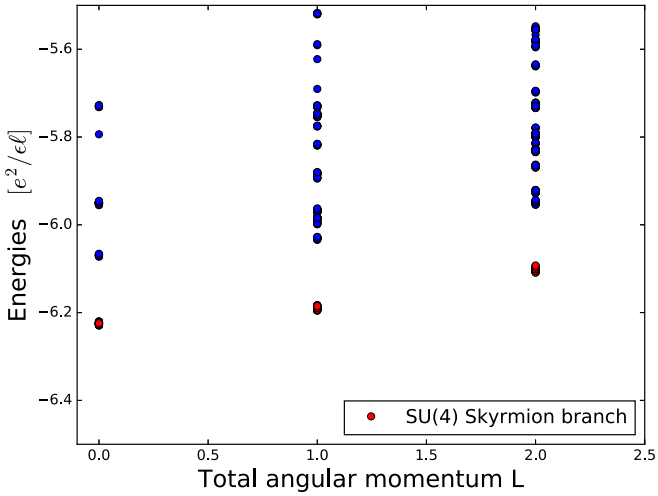

FIG. 7. The $\nu = 0$ case: energy spectrum for nine electrons at $N_\phi = 4$ on a sphere leading to one hole skyrmion. The corresponding quantum states have $L = 0, 1, 2$ marked by red dots. The degeneracies are those predicted by standard skyrmion counting extended to four flavors. The eigenvalues are computed in the AF phase with $\theta = 0.6\pi$ and $\tilde{g} = 0.01$ (chosen for readability). The important observation is that there are no new states that change the overall picture. All new physics is entirely contained in the multiplet structure of the skyrmion branch. This observation is valid for all values of θ in the F and AF phases we explored and up to $\tilde{g} \lesssim 1$.

give the ground-state quantum numbers as a function of $\tilde{g}$. This phenomenon happens both in the F and the AF phases. If we plot the critical anisotropies as a function of system size, we observe that fixing $\tilde{g}$ and increasing the system size leads always to the ground state with maximal L value given by

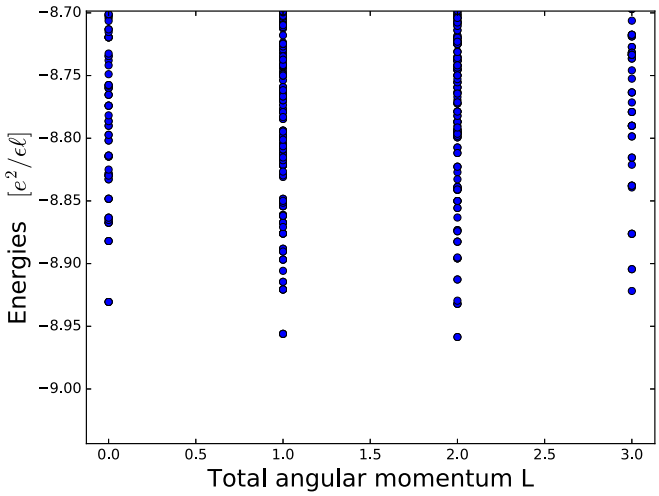

FIG. 8. Lower part of the energy spectrum for 13 electrons at $N_\phi = 6$ on a sphere leading to one hole skyrmion. The skyrmion states have $L = 0, 1, 2, 3$. The eigenvalues are computed in the AF phase with $\theta = 0.6\pi$ and $\tilde{g} = 0.3$. The ground state has no longer $L = 0$. Indeed, with this choice of anisotropy and size it has orbital angular momentum $L = 2$ meaning that the skyrmion has now a finite size instead of spreading all over the sphere. This is in the absence of a Zeeman field.

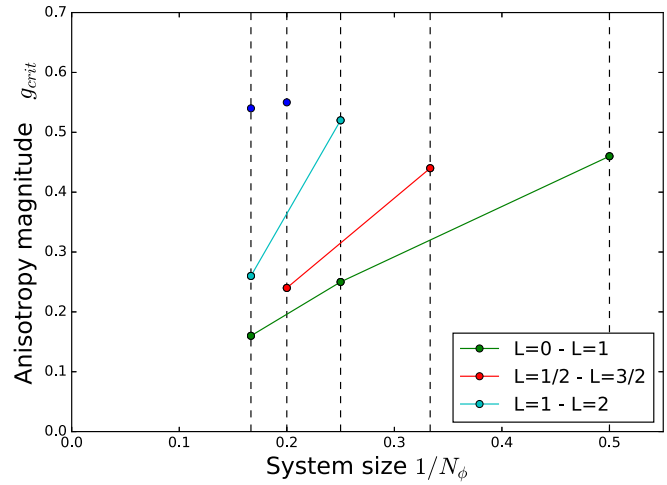

FIG. 9. The critical anisotropies separating ground state with distinct orbital angular momentum on the spherical geometry as a function of system size. Below, the green line systems with $N_\phi = 2, 4, 6$ have a $L = 0$ ground state and $L = 1$ above. The blue line marks the separation between $L = 1$ and 2 for $N_\phi = 4, 6$. System with odd $N_\phi = 3, 5$ have half-integer orbital angular momentum and have the minimal value $L = \frac{1}{2}$ below the red line and $L = \frac{3}{2}$ above. Extrapolations of these boundaries are all zero. At fixed anisotropy $\tilde{g}$ this means that a large enough system has a ground state with maximal L, the end point of the skyrmion branch. Calculations were performed in the AF phase with $\theta = 0.6\pi$ and similar results hold for $\theta = 0.2\pi$ in the F phase.

$N_\phi/2$ (see Fig. 9). Moving toward large system size always leads to a skyrmion state with the maximal value of L. In the case of the SU(2) skyrmion, that would mean complete polarization. Here, it is not the case. Indeed, the value of K is now decoupled from the spin value which is determined by the level ordering inside the IR with this maximal L value.

So, at fixed $\tilde{g}$ we observe that the system when it is large enough has a localized skyrmion excitation. The magnetization process that takes place now is similar to the case of $\nu = \pm 1$. It is the Zeeman splitting of the multiplet $L = N_\phi/2$ that governs the magnetization. There, we find the difference between F and AF phases. In the F case the lowest-lying state at $L = N_\phi/2$ has maximal spin so the system is always fully polarized: charged excitations are fully polarized quasiparticles. On the contrary, in the AF phase there is progressive magnetization with increasing Zeeman energy. It is important to note that due to the multicomponent nature of the system, the spatial and the magnetization are no longer coupled, contrary to spin SU(2) skyrmions. To fully spin polarize the

TABLE III. The angular momentum of the ground state of a skyrmion state with $N_\phi = 6$ and $N = 13$ electrons as a function of anisotropy scale $\tilde{g}$ for $\theta = 0.6\pi$. If one increases the system size at fixed anisotropy, the ground state ends up at $L = 0$.

$\tilde{g}$	0.1	0.2	0.3	0.4	0.5	0.6
L	0	1	2	2	2	3

skyrmion, we estimate that the Zeeman energy should be

$$g_L \mu_B B_{\text{sat}} \approx 0.16\, \tilde{g} \times [e^2/(\epsilon \ell_B)] = 0.16\, (g/\ell_B^2) \qquad (24)$$

for $\theta = 0.6\pi$. This value is approximately three times higher than in the case of the $\nu = -1$ electron skyrmion.

VI. CONCLUSIONS

We have performed a study of skyrmion physics in monolayer graphene for Landau level filling factors $\nu = \pm 1, 0$ by use of exact diagonalization on the spherical geometry. The lattice-scale anisotropies that break the SU(4) spin/valley symmetry have been incorporated by a simple local effective interaction with two parameters. The skyrmion physics for $\nu = \pm 1$ on one side and $\nu = 0$ on the other side has the specific feature that the ground-state angular momentum on the sphere is not related to the spin polarization contrary to ordinary SU(2) skyrmions. We have shown that state counting from straightforward application of SU($N = 4$) skyrmion theory is correct, i.e., there are no additional states in the low-energy spectrum.

In the case of $\nu = -1$ the hole skyrmion does not feel the anisotropies and is an infinite-size spin-polarized valley skyrmion. The denser electron skyrmion on the contrary has a different behavior in the AF and F phases. In the F phase, it is also fully polarized and infinite sized so essentially similar to the hole case. In the AF phase, the electron skyrmion is still of infinite size but is unpolarized at small Zeeman energy. A critical value of the ratio of Zeeman energy versus Coulomb energy is necessary to obtain a fully polarized state. This is in agreement with the measurements of Ref. [53] at $\nu = -1$ that give evidence for spin flips as seen by a gap increase with increasing total magnetic field. This means that these measurements are in the AF state.

In the case of $\nu = 0$, the counting of states from generalized skyrmion theory is still correct but there is a change of behavior for the ground-state quantum numbers. Indeed, we find that for large enough system size, the skyrmion is always in a maximally localized state in real space with a size of the order of a magnetic length. In the F phase, the skyrmion is fully spin polarized, while in the AF phase there is a nontrivial magnetization process and a finite Zeeman energy is required to obtain a fully spin-polarized quasiparticle. Again, the polarization mechanism is disconnected from the spatial extent of the skyrmion. The competition between anisotropies and Zeeman effect means also that there is no longer a universal scaling of skyrmion physics with the ratio of Zeeman energy to Coulomb energy. Our results are summarized in Table IV.

Recent experiments [53] have measured transport gaps as a function of the total magnetic field applied to the sample and also as a function of the perpendicular component of the field by using a tilted-field configuration. This allows to separately control the Coulomb energy (sensitive only to the perpendicular component of the field) and the Zeeman energy (sensitive to the total field). The transport gap is expected to be due to a skyrmion-antiskyrmion pair excitation. The field dependence of the gap at $\nu = -1$ has been measured [53] and is steeper as a function of the total field than expected for a simple electron-hole pair. This is evidence for extra spin flips involved in the excitations. This is exactly what we expect from our results provided the sample is in the AF phase (see Table IV). The AF phase is also the explanation of the conductance transition observed at very large fields [55] so this is a coherent picture. In the anisotropy model we use, it is important to note that contrary to the standard clean skyrmion model there is no universal scaling as a function of the ratio of Zeeman energy to Coulomb energy. Indeed, the Coulomb energy is replaced by the anisotropy energy (provided it is small enough). Deviations from the standard clean skyrmion scaling have been observed in Ref. [53] but only for $\nu = -4$. It remains to be seen if this is also true in the central Landau level. We have obtained in Sec. IV an estimate for the magnetic field required to fully polarize the skyrmions. If we ask that for the largest field used in Ref. [53], $B = 35$ T, the skyrmion is not fully polarized, this requires $g_L \mu_B (B = 35\ \text{T}) \lesssim 0.05 (g/\ell_B^2)$, hence, an anisotropy energy scale $g/\ell_B^2 \gtrsim 800$ K. Such a value is large but still below the Coulomb energy scale $\approx$1500 K using $\epsilon = 2.5$ as appropriate for graphene on hexagonal boron nitride substrate. The idea behind the introduction of the simple local model (4) that anisotropies are a small perturbation that selects the true ground state within the SU(4) manifold is thus still valid. This estimate calls for more attempts to study the magnitude of the anisotropies, notably to find an estimate of the θ parameter distinguishing $g_\perp$ and g_z.

While the diagonalizations we have performed give information about skyrmion quantum numbers, they cannot lead to reliable estimates of the associated gaps, but only orders of magnitude. In addition, it is hard to access the whole range of θ parameter because there are additional degeneracies at high-symmetry points like the F/AF boundary. A strategy would be to construct Hartree-Fock wave functions that can be evaluated for very large systems and with the correct quantum numbers. We have found that this is not easy because simple generalizations of Eq. (8) are not sensitive to anisotropies. While we have concentrated on the central Landau levels, there is also skyrmion physics in the higher Landau levels that requires detailed investigation. Another open question is the

TABLE IV. Summary of results for the skyrmions called here *h*-sk and *e*-sk for both phases considered in this work. Results for filling factor $\nu = +1$ are obtained from the $\nu = -1$ by exchanging hole and electron due to the particle-hole symmetry.

	AF	F
$\nu = -1$	*h*-sk: infinite-sized valley, fully spin polarized *e*-sk : infinite-sized, partially spin polarized	*h*-sk : inifinite-sized valley, fully spin polarized *e*-sk : infinite-sized, fully spin polarized
$\nu = 0$	Localized, partially spin polarized	Localized, fully spin polarized

role of Landau level mixing which is certainly quantitatively important in monolayer graphene. This is an effect which cannot be straightforwardly included in ED studies since the Fock space is already very large due to the spin and valley degeneracies, so adding more levels is not feasible. However, such effects can be treated in the Hartree-Fock approximation (see, e.g., Refs. [57,59]. To implement this approach, one has to write skyrmion wave functions generalizing Eq. (12). While this will change energetics, it will not change our most important finding, i.e., the decoupling of the magnetization process and the spatial profile of the skyrmions.

ACKNOWLEDGMENTS

We acknowledge discussions with M. Bauer and I. Sodemann. Thanks are due to T. Mizusaki for collaboration at an early stage of this project. Calculations were performed on the Cobalt computer operated by GENCI-CCRT.

[1] K. S. Novoselov *et al.*, Science **306**, 666 (2004); Y. Zhang, J. P. Small, M. E. S. Amori, P. Kim, Phys. Rev. Lett. **94**, 176803 (2005); C. Berger *et al.*, J. Phys. Chem. B **108**, 19912 (2004).

[2] K. S. Novoselov, A. K. Geim, S. V. Morozov, D. Jiang, M. I. Katsnelson, I. V. Grigorieva, S. V. Dubonos, and A. A. Firsov, Nature (London) **438**, 197 (2005).

[3] Y. Zhang, Y.-W. Tan, H. L. Stormer, and P. Kim, Nature (London) **438**, 201 (2005).

[4] Y. Zhang, Z. Jiang, J. P. Small, M. S. Purewal, Y.-W. Tan, M. Fazlollahi, J. D. Chudow, J. A. Jaszczak, H. L. Stormer, and P. Kim, Phys. Rev. Lett. **96**, 136806 (2006).

[5] Y. Barlas, K. Yang, and A. H. MacDonald, Nanotechnology **23**, 052001 (2012).

[6] K. Yang, S. Das Sarma, and A. H. MacDonald, Phys. Rev. B **74**, 075423 (2006).

[7] E. H. Rezayi, Phys. Rev. B **36**, 5454 (1987).

[8] E. H. Rezayi, Phys. Rev. B **43**, 5944 (1991).

[9] S. L. Sondhi, A. Karlhede, S. A. Kivelson, and E. H. Rezayi, Phys. Rev. B **47**, 16419 (1993).

[10] K. Moon, H. Mori, K. Yang, S. M. Girvin, A. H. MacDonald, L. Zheng, D. Yoshioka, and S. C. Zhang, Phys. Rev. B **51**, 5138 (1995).

[11] K. Yang, K. Moon, L. Belkhir, H. Mori, S. M. Girvin, A. H. MacDonald, L. Zheng, and D. Yoshioka, Phys. Rev. B **54**, 11644 (1996).

[12] M. Abolfath, J. J. Palacios, H. A. Fertig, S. M. Girvin, and A. H. MacDonald, Phys. Rev. B **56**, 6795 (1997).

[13] H. A. Fertig, L. Brey, R. Côté, and A. H. MacDonald, Phys. Rev. B **50**, 11018 (1994).

[14] H. A. Fertig, L. Brey, R. Côté, A. H. MacDonald, A. Karlhede, and S. L. Sondhi, Phys. Rev. B **55**, 10671 (1997).

[15] N. R. Cooper, Phys. Rev. B **55**, R1934(R) (1997).

[16] R. Côté, A. H. MacDonald, L. Brey, H. A. Fertig, S. M. Girvin, and H. T. C. Stoof, Phys. Rev. Lett. **78**, 4825 (1997).

[17] X.-G. Wu and S. L. Sondhi, Phys. Rev. B **51**, 14725 (1995).

[18] See contributions by S. M. Girvin and A. H. MacDonald, and by J. P. Eisenstein in Ref. [19].

[19] *Perspectives in Quantum Hall Effects*, edited by S. Das Sarma and A. Pinczuk (Wiley, New York, 1997).

[20] S. E. Barrett, G. Dabbagh, L. N. Pfeiffer, and K. W. West, and R. Tycko, Phys. Rev. Lett. **74**, 5112 (1995); A. Schmeller, J. P. Eisenstein, L. N. Pfeiffer, and K. W. West, *ibid.* **75**, 4290 (1995); E. H. Aifer, B. B. Goldberg, and D. A. Broido, *ibid.* **76**, 680 (1996); V. Bayot, E. Grivei, S. Melinte, M. B. Santos, and M. Shayegan, *ibid.* **76**, 4584 (1996); V. Bayot, E. Grivei, J.-M. Beuken, S. Melinte, and M. Shayegan, *ibid.* **79**, 1718 (1997); D. R. Leadley, R. J. Nicholas, D. K. Maude, A. N. Utjuzh, J. C. Portal, J. J. Harris, and C. T. Foxon, *ibid.* **79**, 4246 (1997); J. L. Osborne, A. J. Shields, M. Y. Simmons, N. R. Cooper, D. A. Ritchie, and M. Pepper, Phys. Rev. B **58**, R4227(R) (1998); S. Melinte, E. Grivei, V. Bayot, and M. Shayegan, Phys. Rev. Lett. **82**, 2764 (1999); J. H. Smet, R. A. Deutschmann, F. Ertl, W. Wegscheider, G. Abstreiter, and K. v. Klitzing, *ibid.* **92**, 086802 (2004); G. Gervais, H. L. Stormer, D. C. Tsui, P. L. Kuhns, W. G. Moulton, A. P. Reyes, L. N. Pfeiffer, K. W. Baldwin, and K. W. West, *ibid.* **94**, 196803 (2005).

[21] D. P. Arovas, A. Karlhede, and D. Lilliehook, Phys. Rev. B **59**, 13147 (1999).

[22] R. L. Doretto and C. M. Smith, Phys. Rev. B **76**, 195431 (2007).

[23] N. Shibata and K. Nomura, Phys. Rev. B **77**, 235426 (2008).

[24] D. A. Abanin, B. E. Feldman, A. Yacoby, and B. I. Halperin, Phys. Rev. B **88**, 115407 (2013).

[25] K. Hasebe and Z. F. Ezawa, Phys. Rev. B **66**, 155318 (2002); Z. F. Ezawa, G. Tsitsishvili, and K. Hasebe, *ibid.* **67**, 125314 (2003).

[26] Z. F. Ezawa and G. Tsitsishvili, Phys. Rev. D **72**, 085002 (2005).

[27] G. Tsitsishvili and Z. F. Ezawa, Phys. Rev. B **72**, 115306 (2005).

[28] C. Töke and J. K. Jain, J. Phys.: Condens. Matter **24**, 235601 (2012).

[29] Y. Lian, A. Rosch, and M. O. Goerbig, Phys. Rev. Lett. **117**, 056806 (2016).

[30] Y. Lian and M. O. Goerbig, Phys. Rev. B **95**, 245428 (2017).

[31] L. Brey, H. A. Fertig, R. Côté, and A. H. MacDonald, Phys. Rev. B **54**, 16888 (1996).

[32] L. Brey, H. A. Fertig, R. Côté, and A. H. MacDonald, Phys. Rev. Lett. **75**, 2562 (1995).

[33] K. Yang and S. L. Sondhi, Phys. Rev. B **54**, R2331(R) (1996).

[34] A. G. Green, Phys. Rev. B **61**, R16299(R) (2000).

[35] E. H. Rezayi and S. L. Sondhi, Int. J. Mod. Phys. **13**, 2257 (1999).

[36] J. Sinova, S. M. Girvin, T. Jungwirth, and K. Moon, Phys. Rev. B **61**, 2749 (2000).

[37] S. Sankararaman and R. Shankar, Phys. Rev. B **67**, 245102 (2003).

[38] A. V. Ferrer, R. L. Doretto, and A. O. Caldeira, Phys. Rev. B **70**, 045319 (2004).

[39] O. Bar, M. Imboden, and U. J. Wiese, Nucl. Phys. B **686**, 347 (2004).

[40] A. H. MacDonald, H. A. Fertig, and L. Brey, Phys. Rev. Lett. **76**, 2153 (1996).

[41] X. C. Xie and S. He, Phys. Rev. B **53**, 1046 (1996).

[42] J. J. Palacios, D. Yoshioka, and A. H. MacDonald, Phys. Rev. B **54**, R2296(R) (1996).

[43] A. H. MacDonald and J. J. Palacios, Phys. Rev. B **58**, R10171(R) (1998).
[44] A. Wojs and J. J. Quinn, Phys. Rev. B **66**, 045323 (2002).
[45] Y. P. Shkolnikov, S. Misra, N. C. Bishop, E. P. De Poortere, and M. Shayegan, Phys. Rev. Lett. **95**, 066809 (2005).
[46] J. Alicea and M. P. A. Fisher, Phys. Rev. B **74**, 075422 (2006).
[47] M. O. Goerbig, R. Moessner, and B. Douçot, Phys. Rev. B **74**, 161407(R) (2006).
[48] M. Kharitonov, Phys. Rev. B **85**, 155439 (2012).
[49] M. Kharitonov, Phys. Rev. B **86**, 075450 (2012).
[50] F. Wu, I. Sodemann, Y. Araki, A. H. MacDonald, and Th. Jolicoeur, Phys. Rev. B **90**, 235432 (2014).
[51] I. F. Herbut, Phys. Rev. B **75**, 165411 (2007).
[52] J. Jung and A. H. MacDonald, Phys. Rev. B **80**, 235417 (2009).
[53] A. F. Young, C. R. Dean, L. Wang, H. Ren, P. Cadden-Zimansky, K. Watanabe, T. Taniguchi, J. Hone, K. L. Shepard, and P. Kim, Nat. Phys. **8**, 550 (2012).
[54] P. Maher, C. R. Dean, A. F. Young, T. Taniguchi, K. Watanabe, K. L. Shepard, J. Hone, and P. Kim, Nat. Phys. **9**, 154 (2013).
[55] A. F. Young, J. D. Sanchez-Yamagishi, B. Hunt, S. H. Choi, K. Watanabe, T. Taniguchi, R. C. Ashoori, and P. Jarillo-Herrero, Nature (London) **505**, 528 (2014).
[56] K. Nomura and A. H. MacDonald, Phys. Rev. Lett. **96**, 256602 (2006).
[57] B. Roy, M. P. Kennett, and S. D. Sarma, Phys. Rev. B **90**, 201409(R) (2014).
[58] L. Sheng, D. N. Sheng, F. D. M. Haldane, and L. Balents, Phys. Rev. Lett. **99**, 196802 (2007).
[59] B. Feshami and H. A. Fertig, Phys. Rev. B **94**, 245435 (2016).